

RESEARCH

Open Access



Removal of Isolan Dark Blue 2SGL-01 from aqueous solutions onto calcined and uncalcined (Mg-Zn)/(Al-Fe)-(CO₃)/Cl layered double hydroxides

Ibrahim M. M. Kenawy¹, Medhat A. H. Hafez¹, Abdalla A. Mousa², Zainab Abd Elbary^{1*}  and Khaled S. Abou-El-Sherbini³

Abstract

The adsorption process of the industrialized dye Isolan Dark Blue 2SGL-01 (IDB) onto (Mg-Zn)/(Al-Fe)-(CO₃)/Cl layered double hydroxides (LDHs) coded LDH21 and LDH22 and its calcined products CLDHs (CLDH21 and CLDH22), respectively, was investigated. The characterization of LDHs and CLDHs before and after loading with IDB by Fourier transform infrared, scanning electron microscope and surface area measurements showed a typical hydroxalite structure and confirmed the loading of IDB. The adsorption parameters; initial pH, shaking time, adsorbent dose, initial concentration of IDB dye and temperature were studied. The optimum conditions for IDB adsorption were pH 4.3 and shaking time 3 h. A complete removal of IDB (> 99%) was achieved using a dosage of 2.0 g L⁻¹ CLDHs or LDH22, and 3.0 g L⁻¹ of LDH21. The adsorption processes were suggested to be best described by the pseudo-second order kinetics and Langmuir-type adsorption isotherm with monolayer capacities of 75, 91, 427 and 530 mg g⁻¹, onto LDH21, LDH22, CLDH21 and CLDH22, respectively. The loaded IDB was recovered from LDHs and CLDHs adsorbent using Na₂CO₃. CLDH22 showed best adsorption capacity of 530 mg g⁻¹. Its adsorption thermodynamic parameters $\Delta G_{adsorption}$, $\Delta H_{adsorption}$ and $\Delta S_{adsorption}$ indicated that the adsorption processes were spontaneous and endothermic in nature. CLDH22 was successfully applied for the removal of IDB from simulated dyeing process with removal efficiency 97%.

Keywords: Layered double hydroxides, Calcined layered double hydroxides, Isolan Dark Blue 2SGL-01, Adsorption, Wastewater treatment

Introduction

Environmental pollution posed by synthetic dyes from many industries such as textile manufacturing, leather tanning, cosmetics and electroplating is a serious problem. These ionic dyes are considered as one of the important classes of the organic pollutants, once they enter water; it is no longer safe and sometimes difficult to be treated. Owing to their complex molecular structure containing recalcitrant organic molecules which makes

them more stable and resistant to aerobic degradation. They are often toxic, even carcinogenic and non-degradable that threatens the living organisms [1, 2].

The Isolan Dark Blue 2SGL-01 (IDB) is a 1:2 metal complex, mono-sulphonated dye. This IDB dye contains 8.35% chromium(III) metal [3]. The presence of the heavy metal ion chromium(III) in the structure of IDB dye imposes an additional threat to the environment rather than the toxicity of the organic substrates if its effluents are released into water bodies without treatment. The tendency of Cr(III) to precipitate as amorphous hydroxide, excessive quantities of trivalent Cr(III) may

* Correspondence: isis_eg@yahoo.com

¹Department of Chemistry, Mansoura University, Mansoura 35516, Egypt
Full list of author information is available at the end of the article



© The Author(s). 2021 **Open Access** This article is licensed under a Creative Commons Attribution 4.0 International License, which permits use, sharing, adaptation, distribution and reproduction in any medium or format, as long as you give appropriate credit to the original author(s) and the source, provide a link to the Creative Commons licence, and indicate if changes were made. The images or other third party material in this article are included in the article's Creative Commons licence, unless indicated otherwise in a credit line to the material. If material is not included in the article's Creative Commons licence and your intended use is not permitted by statutory regulation or exceeds the permitted use, you will need to obtain permission directly from the copyright holder. To view a copy of this licence, visit <http://creativecommons.org/licenses/by/4.0/>.

accumulate in living causing damage aquatic organisms and disruption of the food chain [4]. Hence, it is mandatory to treat wastewaters containing IDB dye before its discharge into environment.

Several recent treatment methodologies and technologies are applied to remove anionic hazards from water effluents such as electrocoagulation, ultrafiltration, nanofiltration, photocatalytic degradation, adsorption, solid phase extraction (SPE) and biological treatment [5]. However, most of these techniques have several limitations of high cost, low efficiency, production of sludge, non-recoverability, slowness, inapplicability to a wide range of pollutants and/or the generation of secondary pollution. SPE arose as a conventional technique and highly efficient physico-chemical treatment process for the removal of organic pollutants from their aqueous matrices [6]. The main advantages of this technique are its greater flexibility in the design of the aimed adsorbent for the targeted pollutant, high efficiency, reusability of material, easy handling and low cost.

Layered double hydroxides (LDHs) are a group SPE sorbents with a brucite-like $M^{2+}_{(1-x)}/M^{3+}_x$ structure intercalated with anions ($x/n A^{n-}$) for charge compensation [7]. They are potentially cheap sorbents for a diverse number of anions with high anion-exchange capacity. They are also easily synthesized, selective, regenerative and eco-friendly structure [8]. Their calcination products (CLDHs) restore the LDH structure, once being hydrolysed, with larger surface area and better adsorption efficiency [9]. Many studies reported the use of LDHs and CLDHs for organic dyes separation. Ni/Mg/Al LDH and its calcined were employed for Congo Red dye removal with maximum uptakes 287 and 1247 mg g^{-1} , respectively [10]. In addition, Co/Fe LDH was synthesized with various ratios 2:1, 3:1 and 4:1 to remove Methyl Orange dye from aqueous media, with uptake capacities 77–135 mg g^{-1} , respectively [11]. Moreover, Mg/Al LDH and its modified with 2-hydroxyethylammonium acetate (HEAA) were prepared to remove Acid Red 27 and Direct Red 23 dyes with highest capacities 74 and 420 mg g^{-1} , respectively [12]. Also, Mg/Al- CO_3 LDH with Mg/Al ratio 2:1 was organized to sorb different red dyes from the solution. Uptakes of Reactive Red, Congo Red and Acid Red dyes were 95, 37 and 127 mg g^{-1} , respectively [13]. Congo Red dyes was also sorbed onto modified acetate intercalated layered Zn/Y hydroxide with dodecylsulfate with adsorption capacities 77 and 96 mg g^{-1} , respectively [14]. Methyl Orange dye adsorption was investigated onto Mg/Al-LDH surface and showed that the adsorption capacity was 120 mg g^{-1} [15]. Also, calcined Mg/Fe (2:1) was utilized to remove Methyl Orange dye with maximum uptake 160 mg g^{-1} [16]. Additionally, Au-Pd nanoparticles (1% Au-Pd) immobilized on NiFeCO_3 -LDH (3:1) was found to be the best

adsorbent degrading about 64% of the Orange II dye (64 mg g^{-1}) [17].

Recently, the synthesis of a series of LDH and CLDH compositions of (Mg,Zn)/(Al,Fe)-(CO_3 ,Cl) with magnetic properties was reported which gave promising adsorption capacities for anionic hazards attributed to stabilizing structure by isostructural substitution of approximately 20% of Mg and Al with Zn and Fe, respectively [18]. Their adsorption behavior of LDHs and CLDHs coded LDH21, LDH22, CLDH21 and CLDH22 towards IDB dye has not previously been detailed. The present work is carried out to optimize the parameters affecting the adsorption process of IDB dye on these most efficient adsorbents in order to enhance their removal efficiency. Also, the process will be applied for the removal of IDB dye from polluted sample.

Materials and methods

Materials

Magnesium chloride (MgCl_2 , 99%), zinc chloride (ZnCl_2 , 97%), aluminum chloride ($\text{AlCl}_3 \cdot 6\text{H}_2\text{O}$, 97%), ferric chloride (FeCl_3 , 98%), NaOH and Na_2CO_3 were obtained from ALPHA Chemika, Mumbai-India. IDB dye (molecular formula $\text{C}_{20}\text{H}_{16}\text{CrN}_2\text{O}_{11}\text{S}_2\text{Na}_2$ and molecular weight 622.5 g mol^{-1}) and lyogen[®]NH (leveling agent) were obtained from DyStar colors company, Raunheim, Germany.

Synthesis of the adsorbents

The co-precipitation procedure and characterization of LDH21 and LDH22 were previously described [18]. To get LDH21 or LDH22, a solution of Mg(II), Zn(II), Al(III) and Fe(III) chlorides with initial metal molar ratios of 2.4:0.6:0.9:0.1 or 2.4:0.6:0.8:0.2, respectively, was prepared. LDHs were precipitated through immediate dropwise addition of 100 mL of a total of 2.5 M of the mixture of the metal chlorides to a basic carbonate solution (NaOH, Na_2CO_3). The suspension was adjusted at pH = 9.9, kept at 75–80 °C for 7 d and then filtered. The resulting precipitate was washed repeatedly for 9 times with bi-distilled water, frequently dried at 75 °C for 2 d, kept in desiccator. The initial and final elemental compositions of LDHs are shown in Table 1. Calcined LDH (CLDH) was obtained via thermal treatment of LDH materials at 500 °C for 2.5 h, vacuum cooled at 25 °C and kept in desiccator and coded CLDH21 and CLDH22, respectively.

Micro-structural characterization

Fourier transform infrared (FTIR) spectra were determined with a Nicolet iS10, Thermo-Fisher Scientific, USA, by potassium bromide pellets. Specific surface area (S_{BET}) was recorded on a BELSORP-mini II, BEL Japan, with nitrogen at 77 K. Prior to measurement, the

Table 1 Proportion of salts used for the synthesis of LDHs and their codes

Sample code	Initial molar chloride solutions Mg/Zn/Al/Fe ratio	Final Mg/Zn/Al/Fe/Cl/CO ₃ ratio
LDH21	2.4/0.6/0.9/0.1	2.72/0.72/0.80/0.20/0.26/0.37
LDH22	2.4/0.6/0.8/0.2	2.30/0.56/0.74/0.26/0.29/0.35

sorbents were heated at 115 and 450 °C for LDH22 and CLDH22, respectively, in a vacuum for 12 h to eliminate surface impurities and sorbed water. The scanning electron microscope (SEM) pictures were obtained with Quanta 250.0 FEG with accelerating voltage 30 kV, magnification 14x up to 10⁶x and resolution 1.0 nm at 30 kV for Gun. In, FEI Company, Netherlands. S_{BET} was recorded using the nitrogen molecular cross section BET Method.

UV-Visible adsorption spectrometric measurements were performed by a Unicam (UK) spectrophotometer using a 1.0 cm quartz cell. The IDB dye final concentration solution was recorded on UV-Vis spectrometry at wavelength of 585 nm [3]. Standard known concentration of IDB dye solution was prepared in the range 1–70 mg L⁻¹, that obtain a linear calibration curve. A blank sample without IDB dye and another with dye solution were determined together for each run. All measurements were performed in triplicate runs to validate the observed data. The pH effect study for each sample was adjusted via 0.01 M NaOH or HCl solutions, on a Hanna-8519 Devices, Italy.

Preparation of the stock solutions

The stock of IDB dye solution was prepared by dissolving a weighed dye in bi-distilled water to obtain a 2000 mg L⁻¹ concentration from which appropriate dilutions to various initial concentrations were performed. Application of simulated polluted sample was performed on white nylon fabrics purchased from market to simulate dyeing process.

Optimization of adsorption parameters

Adsorption experiments

LDH21, LDH22, CLDH21 and CLDH22 were used as sorbents for IDB dye by batch mode experiments that were determined in 100 mL glass flask at 30 °C in a closed system. As well, 25 mg of LDHs or CLDHs was shaken for 3 h in 25 mL of IDB solution using 200 and 400 mg L⁻¹ initial concentration for LDHs and CLDHs, respectively, due to their relative high capacity. The initial pH was within range 4.0–10. The suspensions were left for 1 day to confirm equilibration, centrifuged and the final IDB concentration in the aqueous solution was determined spectrometrically.

The shaking time effect, 25 mg of each adsorbent was suspended in 25 mL of IDB solution with 100 mg L⁻¹ initial concentration for LDHs and CLDHs, at the

optimum initial pH, that obtained from the pH effect and the final concentration effect was investigated at various time intervals 5–1440 min.

The sorbent dose effect on the sorption of 25 mL of IDB was carried out by using doses 12–150 mg of different sorbents with an initial concentration 100 or 500 mg L⁻¹ of IDB for LDHs or CLDHs, respectively, at the optimum pH. Then the solutions were shaken for 3 h, centrifuged and the final concentration was determined spectrometrically, which is crucial for its cost-effective application.

The initial concentration effect was investigated by shaking 25 mg of each adsorbent with 25 mL of IDB with an initial concentrations 25–1200 mg L⁻¹, at the optimum pH. The suspensions were then shaken for 3 h, centrifuged and the residual IDB solution was measured spectrometrically.

Effect of temperature was similarly studied for CLDH22, by shaking 25 mg of the adsorbent in 25 mL of dye solution at the optimum initial pH with 300 mg L⁻¹ initial concentration of, at various temperatures 20, 25, 30 and 35 °C ± 2 in thermostated baths. Then the suspensions were shaken for 3 h, centrifuged and the final IDB dye concentration was determined spectrometrically.

Adsorption capacity (q_e) of IDB onto LDHs or CLDHs at equilibrium (q_e , mg g⁻¹) was estimated using Eq. (1):

$$q_e = \frac{(C_i - C_e)}{m} V \text{ (mg g}^{-1}\text{)} \quad (1)$$

C_i and C_e are the aqueous initial and equilibrium concentrations (mg L⁻¹) of IDB. V is the solution volume (L) and m is the sorbent mass (g).

The removal efficiency, E (%), was estimated using Eq. (2):

$$E(\%) = \frac{C_i - C_e}{C_i} \times 100 \text{ (\%)} \quad (2)$$

Desorption study

For desorption studies, 25 mg of LDHs and CLDHs were loaded with IDB, at optimum adsorption conditions: an initial concentration (C_i) 100 mg L⁻¹ in 25 mL, pH 4.0 and shaking time 3 h. Then the precipitates were collected, washed by bi-distilled water and dried at 50 °C. The residual concentration (C_f) in the supernatant liquors was determined after centrifugation. After that, each precipitate was placed in 25 mL of solution

containing either 0.1 M NaCl, 0.1 M NaOH, or 0.1 M and 1.0 M Na₂CO₃ solution with stirring for 30 min at 30 or 50 °C.

The released IDB concentration (C_R) was determined spectrometrically and the recovery efficiency, R (%), was estimated using Eq. (3):

$$R(\%) = \frac{C_i - C_R}{C_i} \times 100 (\%) \quad (3)$$

Removal of IDB dye from simulated contaminated sample

To simulate the dyeing process, 4000 mg of IDB dye and 2000 mg of lyogen[®]NH, as leveling agent, was dissolved in 100 mL bi-distilled water, then 50 g nylon fiber was soaked in this simulated effluent for 30 min. The dyed fiber was removed and the residual IDB dye was diluted to 400 or 100 mg L⁻¹ in 25 mL. CLDH22 or LDH22, respectively, (25 mg) was added to the simulated effluent. The pH was adjusted to 4.3 and shaken for 3 h and the residual concentration was determined in extract liquor after centrifugation. The removal efficiency, E (%), was estimated by Eq. (2).

Results and discussion

Micro-structural characterization

The LDHs, LDH21 and LDH22 were previously investigated with powder X-ray diffraction and thermogravimetric analysis [18]. The layered structure of the selected compositions was previously confirmed which were reported to loss upon calcinations due to the formation of the corresponding oxides. In addition, the following characterization were carried out for LDH22 and the best adsorbent; CLDH22 to confirm their structures.

FTIR

Figure 1a illustrates FTIR spectra of LDHs and CLDHs adsorbent. The LDHs FTIR spectra were fingerprint for hydrotalcite-type materials that emphasize the formation of LDH adsorbents. The strong and broad sorption band detected at 3445–3475 cm⁻¹ relates to the O–H group stretching vibration mode of the surface and interlayer water molecules with the bending mode at the medium intensity band at 1650 cm⁻¹. The bands detected at 768 and 550 cm⁻¹ are corresponding to Mg–OH and Al–OH vibration translation modes, respectively [7]. The bands at 445 cm⁻¹ can be related to the Zn–OH vibration. The CO₃²⁻ species disordered and ordered asymmetric stretching vibration modes were recorded at 1435 and 1368 cm⁻¹, respectively, confirming a split upon deformation that indicates a decrease in symmetry [7]. This was previously related to the Cl⁻ rivaling with CO₃²⁻ ions in the interlayer affecting perturbation of its stacking [18]. These bands and those attributed to metal–OH vibrations

vanished for freshly calcined CLDHs adsorbent, as obtained in Fig. 1a. This confirms that, the CO₃ peak was totally eliminated from the calcined mixed oxide CLDHs.

The FTIR spectra of the loaded LDHs and CLDHs with IDB showed symmetric and asymmetric sulfonate vibration peak at 1047 and 1189 cm⁻¹, respectively (Fig. 1b) confirms the IDB intercalation [19].

SEM

Figure 2 represents SEM micrographs of LDH22 and CLDH22 adsorbents. The characteristic layered texture and the hexagonal crystals of the LDH phase can be seen in Fig. 2a. An obvious disorder and loss of size and crystallinity were observed in the SEM micrograph of CLDH22 (Fig. 2b) owing to the burst loss of CO₂ during calcination which was accompanied with a remarkable increase in the sorbent surface area [18].

S_{BET}

The nitrogen adsorption/desorption isotherms for the LDH22 and CLDH22 adsorbents were reported previously [18, 20] and shown in Fig. 3. The adsorption-desorption isotherms shape is classified as type II with a contribution of type IV by the method of Brunauer Deming Brumaire Teller (according to IUPAC classification). Type II adsorption isotherms are characteristic of macro and non-porous materials whereas the most characteristic feature of the type IV isotherms is the hysteresis loop that is corresponding to the pore condensation occurrence [18, 20]. Hence, a contribution caused by the mesoporous existence (2–50 nm in size) may be determined from the isotherm shape and the presence of a hysteresis loop. As well as, the average pore diameter for LDH22 and CLDH22 were 20.9 and 10.2 nm, respectively, that confirmed the mesoporosity of the sorbents. Additionally, the surface area of LDH22 and CLDH22 were estimated to be 70 and 198 m² g⁻¹, respectively, after the hydrothermal treatment step.

Adsorption optimization parameters

Initial pHs effect

Due to the anion exchange nature of LDHs, only the initial pH of the suspensions was adjusted by HCl and NaOH, which is frequently so called “buffering effect” in literature [19]. Figure 4 shows the effect of initial pHs on adsorption capacity of IDB dye onto LDHs and CLDHs adsorbent. The investigated samples showed highest adsorption efficiencies at ca. 4.3 then gradually decreased with the increase in pH especially for CLDH21 at pH > 7.1. This decrease in sorption capacities may be corresponding to the competitive adsorption of OH⁻ ions with IDB on LDHs and CLDHs as a result of increasing pH value. Consequently, the available sites for IDB dye decreases on the sorbents [20]. Best adsorption capacity (396 mg g⁻¹) was obtained for CLDH22 then CLDH21,

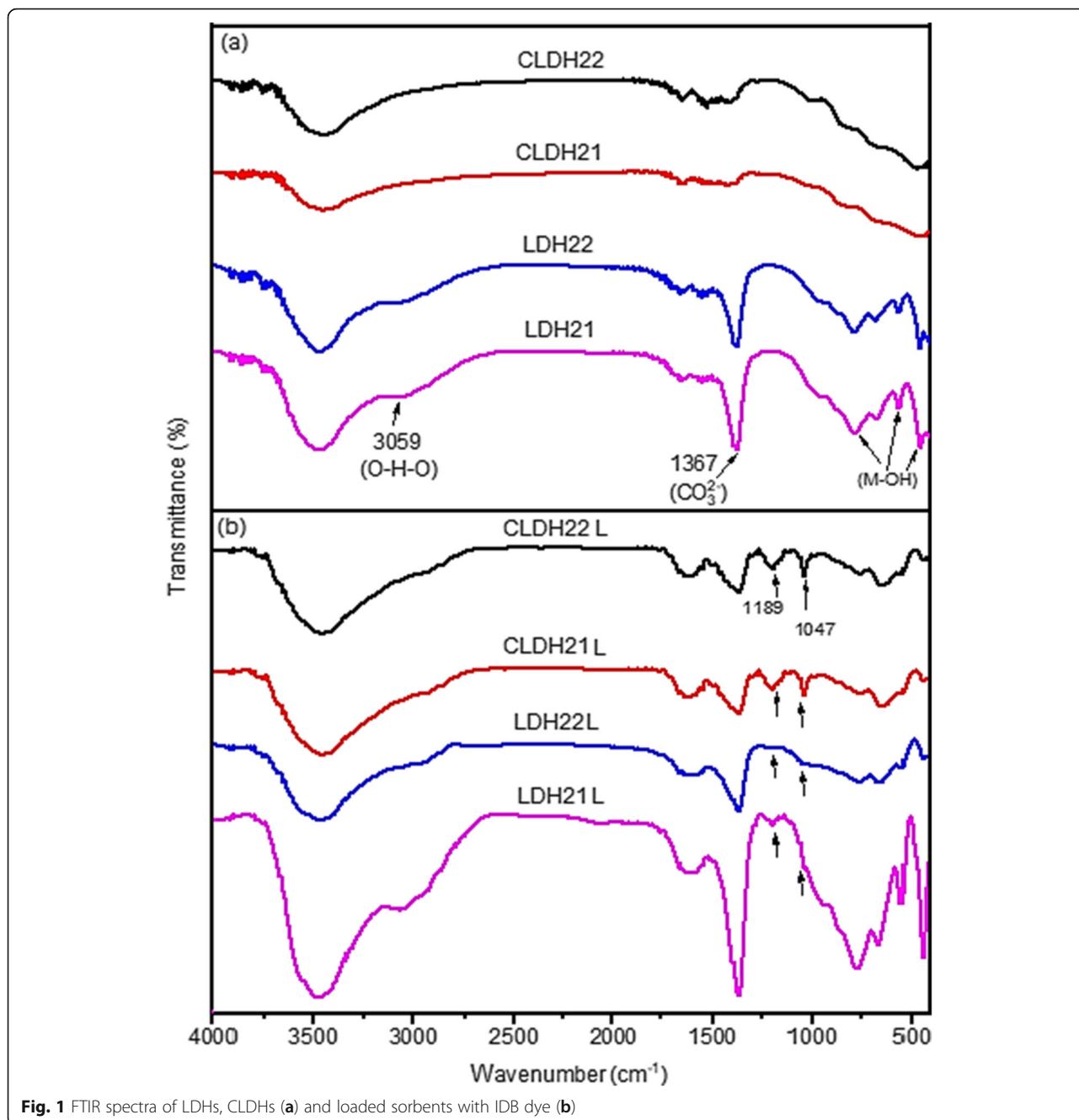
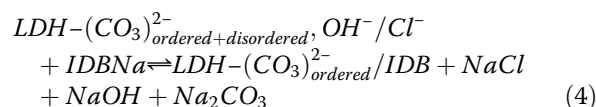


Fig. 1 FTIR spectra of LDHs, CLDHs (a) and loaded sorbents with IDB dye (b)

LDH22 and LDH21. The shown high capacity of CLDHs for IDB compared with LDHs may be attributed to the increase in LDHs surface area due to crater-like formation by the thermal decomposition of the layered structure [21].

Adsorption at pH values lower than 4 was not studied as LDHs and CLDHs adsorbent are generally unstable owing to a partial dissolution occurring in the acidic medium [22]. Consequently, initial pH values 4.41, 4.29, 4.27 and 4.30 were chosen as optimum values for the next studies for LDH21, LDH22, CLDH21 and CLDH22 adsorbents, respectively.

It is important to mention that, the final pH values of all sorbents rose up to 10.7 as a result of the replacement of IDB with $\text{CO}_3^{2-}/\text{Cl}^-$ in case of LDHs according to the ion exchange reaction mechanism Eq. (4):



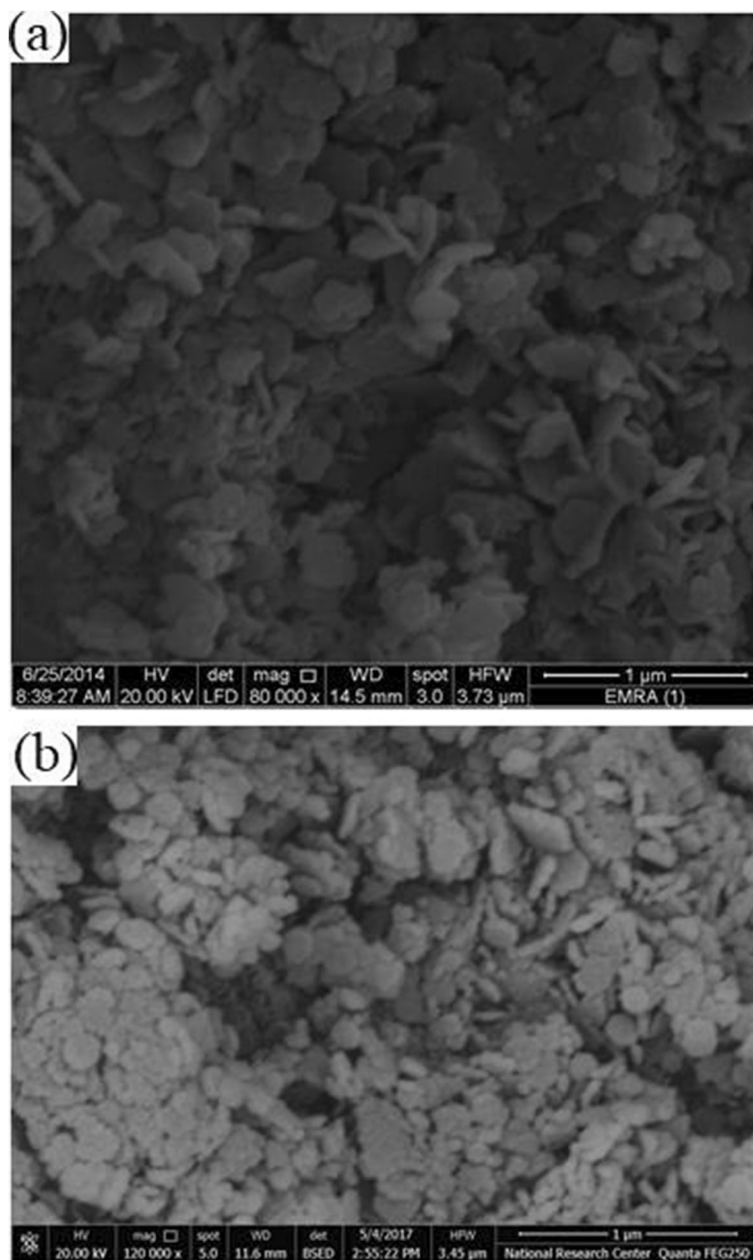
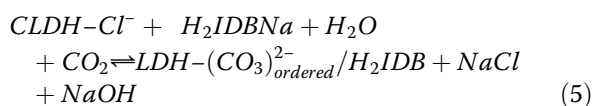


Fig. 2 SEM micrograph of LDH22 (a) and CLDH22 (b)

Whereas, the IDB and CO_3^{2-} (absorbed as CO_2 from air) intercalation could happen to CLDHs according to Eq. (5):

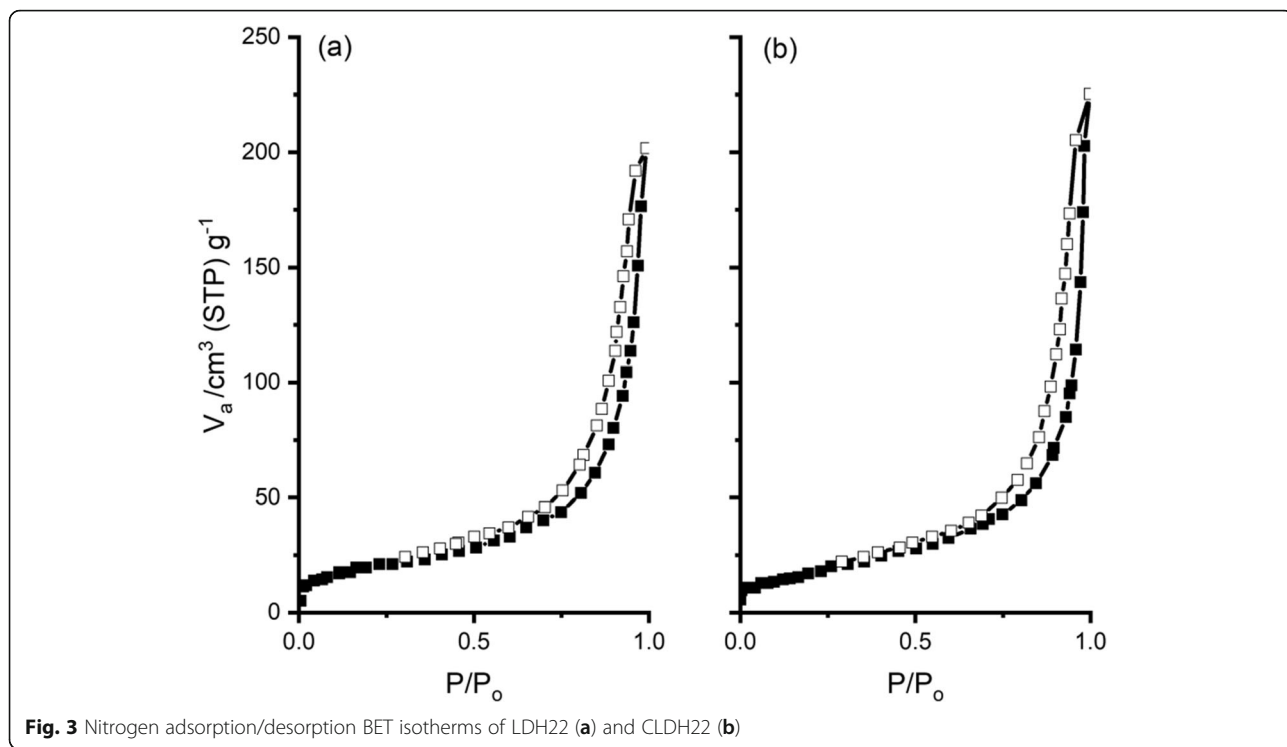


Also, a release of the metal cations and hydroxides from the compounds and their contribution to the intercalation process were reported explaining the

pH increase by the compounds that is fed to the system [23].

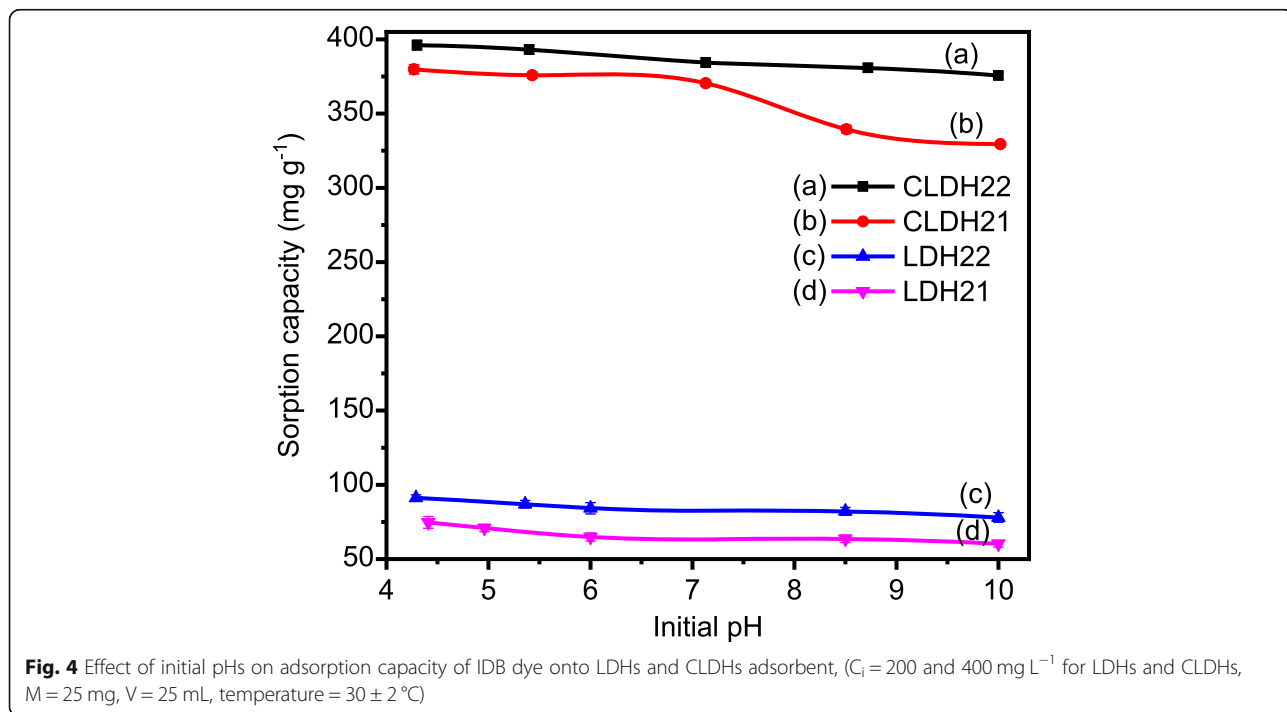
Contact time effect

Figure 5 presents the effect of shaking time on the adsorption capacity of IDB dye onto the investigated LDHs and CLDHs. It was observed that, the IDB sorption capacity values by different sorbents rapidly increased at first, but the rate slowed hereafter as it approached saturation. About 50% of IDB dye was sorbed at 147, 115, 35 and 15 min for LDH21, LDH22, CLDH21 and



CLDH22, respectively. This is mainly owing to the large number of active sites on the sorbents available for the sorption process. The relatively slow uptake kinetics of LDHs is due to the slow ion exchange of the bulky IDB ions with the strongly bonded CO_3^{2-} ions. Whereas, the

adsorption process of CLDHs is faster due to the fast kinetics of intercalation mechanism [24,25]. Finally, the surface sorption sites become completely covered where at this. Point, the slow rate is due to the sorbate transportation from the exterior to the interior sites [26].



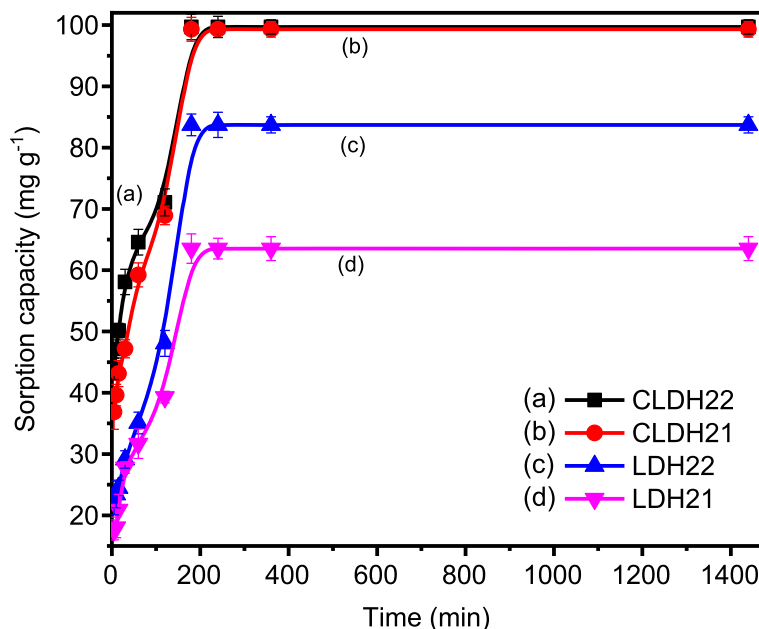


Fig. 5 Effect of shaking time on adsorption capacity of IDB onto LDHs and CLDHs adsorbent, $C_i = 100 \text{ mg L}^{-1}$

Equilibrium was obtained at time of shaking 180 min which is comparable to many LDHs and CLDHs (Table 2). Also, the equilibration time is shorter than common adsorbents such as graphene, graphene oxide and zeolite.

Examination of kinetic models

The obtained uptake time data was treated with three kinetic models. The pseudo 1st order model is mathematically calculated by Eq. (6) [30]:

$$\ln (q_e - q_t) = \ln q_e - k_1 t \tag{6}$$

The pseudo 2nd order model is calculated by Eq. (7) [31]:

$$\frac{t}{q_t} = \frac{1}{k_2 q_e^2} + \frac{1}{q_e} t \tag{7}$$

where k_1 and k_2 are the rate constants of the pseudo 1st order (min^{-1}) and the pseudo 2nd order sorption ($\text{g mg}^{-1} \text{ min}^{-1}$), respectively. Whereas, q_e and q_t represent the IDB amount sorbed (mg g^{-1}) at equilibrium and at time t (min), respectively.

The intraparticle diffusion rate is calculated using Eq. (8) [32]:

$$q_e = k_p \sqrt{t} + C \tag{8}$$

where, k_p is intraparticle diffusion rate constant.

The obtained results in Table 3 show lower values of R^2 and large difference between the experimental and calculated adsorption capacities, q_e in case of the pseudo

1st order reaction and intraparticle diffusion rate models which accordingly failed to describe the adsorption kinetics. On the contrary, the good agreement between the experimental and calculated equilibrium sorption capacity and the high obtained linear regression coefficients ($R^2 \geq 0.995$) based on the pseudo 2nd order model, confirms that this model can better describe the sorption kinetics for IDB on the investigated sorbents. This performance was independent of the experimental effects, i.e. sorbent, initial concentration and pH [30].

Sorbent dose effect

Figure 6 shows the effect of adsorbent dose on adsorption capacity of IDB dye onto the studied LDHs and CLDHs. Applying an optimum dosage of suitable sorbent for sorbate removal is essential for its cost-effective application. It followed the predicted pattern of increasing adsorption capacity as dosage increases and reached complete adsorption of IDB ($E > 99\%$) from aqueous solution. The increase in removal efficiency, is quite obvious with increasing doses of sorbents, at a constant initial concentration. This is owing to the fact that as the vacant surface area increases, larger number of sorption sites is available to sorb IDB and the uptake is enhanced [22].

The complete removal of 100 mg L^{-1} of IDB ($> 99\%$) was obtained at sorbent dose 2.0 g L^{-1} of LDH22 and 3.0 g L^{-1} of LDH21. Due to, the high adsorption capacity of the calcined samples 500 g L^{-1} of IDB was used as initial concentration. A removal efficiency $> 99\%$ was achieved at adsorbent dosage 2.0 g L^{-1} of CLDHs. The observed low needed

Table 2 Capacities of reported LDHs or CLDHs and common sorbents towards sulfonated dyes compared with CLDH22

Adsorbent	Metal Molar ratios (starting salt)	A ⁻	Calcination temperature, °C	Removed dye	Equilibrium time, h	Removal capacity ^a , mg g ⁻¹	Ref.
LDH	Ni/Mg/Al/urea 1:1:1:6 (sulfate/nitrates/ urea)	SO ₄ ²⁻ -/NO ₃ ⁻	180 ^b	Congo Red	2.5	286.5	[10]
CLDH	Ni/Mg/Al/urea 1:1:1:6 (sulfate/nitrates/ urea)	-	600	Congo Red	2.5	1247	[10]
LDH	Co/Fe 2:1,3:1,4:1 (nitrates)	NO ₃ ⁻	65 ^b	Methyl Orange	2	76.5–135	[11]
LDH	Mg/Al 2:1 (nitrates)	CO ₃ ²⁻	100 ^b	Acid Red 27	9	74.4	[12]
LDH	Mg/Al-HEAA 1–3 (nitrates)	C ₂ H ₃ O ₂ ⁻	100 ^b	Direct Red 23	9	420	[12]
LDH	Mg/Al 2:1 (nitrates)	CO ₃ ²⁻	80 ^b	Reactive Red Congo Red Acid Red 1	1	95.0 37.2 127	[13]
LDH	Zn/Y-DS 6:1 (chlorides)	C ₂ H ₃ O ₂ ⁻	-	Congo Red	0.75	96.0	[14]
LDH	Mg/Al 2:1 (nitrates)	CO ₃ ²⁻	200 ^b	Methyl Orange	-	120	[15]
CLDH	Mg/Fe 2:1 (-)	-	500	Methyl Orange	0.5	160	[16]
LDH	Au/Pd/Ni/Fe 1:1:3:1 (nitrates)	CO ₃ ²⁻	105	Orange II	1	64.0	[17]
CLDH10	Mg/Zn/Al 3.67:0.26: 1 (chlorides)	-	450	Isolan Dark Blue 2SGL-01	6	48.7	[18]
LDH20	Mg/Zn/Al 2.67:0.54:1 (chlorides)	CO ₃ ²⁻ -/Cl ⁻	80 ^b	Isolan Dark Blue 2SGL-01	6	11.0	[18]
LDH	Ni/Fe 3:1 (nitrates-sulfate)	NO ₃ ⁻ / SO ₄ ²⁻	180 ^b	Congo red	4	29.4	[27]
CLDH	Ni/Fe 3:1 (nitrates-sulfate)	-	400	Congo red	4	47.4	[27]
ZnO–clay alginate beads	ZnO:C ₆ H ₉ NaO ₇ 1.3:1	-	40 ^b	Congo red	2	78.5	[28]
Lemon citrus peel active carbon	Lemon citrus peels: H ₃ PO ₄	-	500	Rhodamine B Erythrosine B	-	53.0 33.6	[29]
CLDH22	Mg/Zn/Al/Fe 2.30:0.56:0.74:0.26 (chlorides)	-	530	Isolan Dark Blue 2SGL-01	3	530	Present work

^adenotes 'calculated from publication' to ease comparison; ^b denotes hydrothermally aged

dosage of LDH22 and CLDHs that is required to achieve complete removal of IDB is important from the economical aspect.

Initial concentration effect

Figure 7 represents the effect of initial concentration on removal efficiency of IDB onto LDH (a) and CLDH (b)

Table 3 Kinetic model constants and correlation coefficients for adsorption of IDB onto LDHs and CLDHs adsorbent, $C_i = 100 \text{ mg L}^{-1}$

Adsorbent	q_{exp} (mg g^{-1})	Pseudo-first order			Pseudo-second order			Intraparticle diffusion rate	
		k_1 (min^{-1})	$q_{e'} \text{ (cal)}$ (mg g^{-1})	R^2	$k_2 \times 10^{-4}$ ($\text{g mg}^{-1} \text{ min}^{-1}$)	$q_{e' \text{ cal}}$ (mg g^{-1})	R^2	k_p ($\text{g mg}^{-1} \text{ h}^{0.5}$)	R^2
LDH21	63.5	0.010	22.7	0.595	3.435	66.7	0.996	1.43	0.767
LDH22	83.7	0.008	33.6	0.599	2.441	83.3	0.995	2.01	0.767
CLDH21	99.3	0.013	25.8	0.592	3.378	100	0.998	1.93	0.756
CLDH22	99.7	0.012	24.0	0.591	4.049	100	0.998	1.68	0.765

k_1 is the pseudo-first order adsorption rate constant (min^{-1}) and k_2 is the pseudo-second order adsorption rate constant ($\text{g mg}^{-1} \text{ min}^{-1}$)

sorbents. A low uptake with increasing initial concentration was shown for the studied sorbents especially LDHs which caused by an increased ratio of initial number of dye moles to the available surface area. Thus, this results in a decrease in the removal efficiency of adsorbent with increasing the initial concentration of sorbate owing to adsorbent saturation [33].

Fitting of adsorption isotherm models

The most frequently applied equations for describing adsorption isotherms are Langmuir’s and Freundlich’s models. Langmuir’s model can be described as in Eq. (9) [34]:

$$\frac{C_e}{q_e} = \frac{1}{b_L q_{max}} + \frac{C_e}{q_{max}} \tag{9}$$

where, q_{max} is the maximum sorption capacity at monolayer coverage (mg g^{-1}), and b_L is the Langmuir constant

related to adsorption energy (L mg^{-1}). The important characteristics and the feasibility of Langmuir’s isotherm can be determined in terms of a dimensionless equilibrium factor R_L that calculated using Eq. (10):

$$R_L = \frac{1}{1 + b_L C_i} \tag{10}$$

where, R_L value confirms that the isotherm type is irreversible ($R_L = 0$), favorable ($0 < R_L < 1$), linear ($R_L = 1$) or unfavorable ($R_L > 1$).

Freundlich’s model can be described by Eq. (11) [35]:

$$\ln q_e = \ln K_f + \frac{1}{n} \ln C_e \tag{11}$$

The constants associated with the Freundlich’s isotherm model are adsorption capacity (K_f) (mg g^{-1}) and adsorption intensity ($1/n$) being indicative of the extent

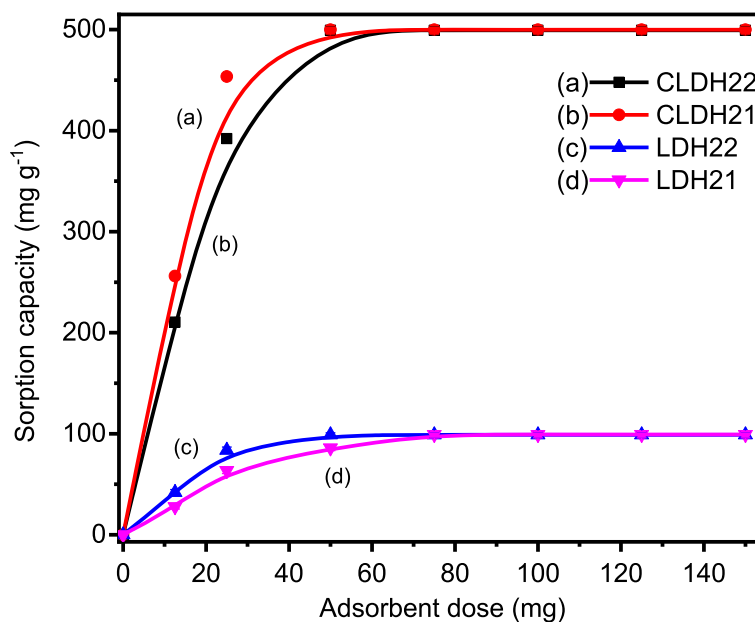


Fig. 6 Effect of adsorbent dose on adsorption capacity of IDB onto LDHs and CLDHs adsorbent, $C_i = 100$ and 500 mg L^{-1} , $V = 25 \text{ mL}$

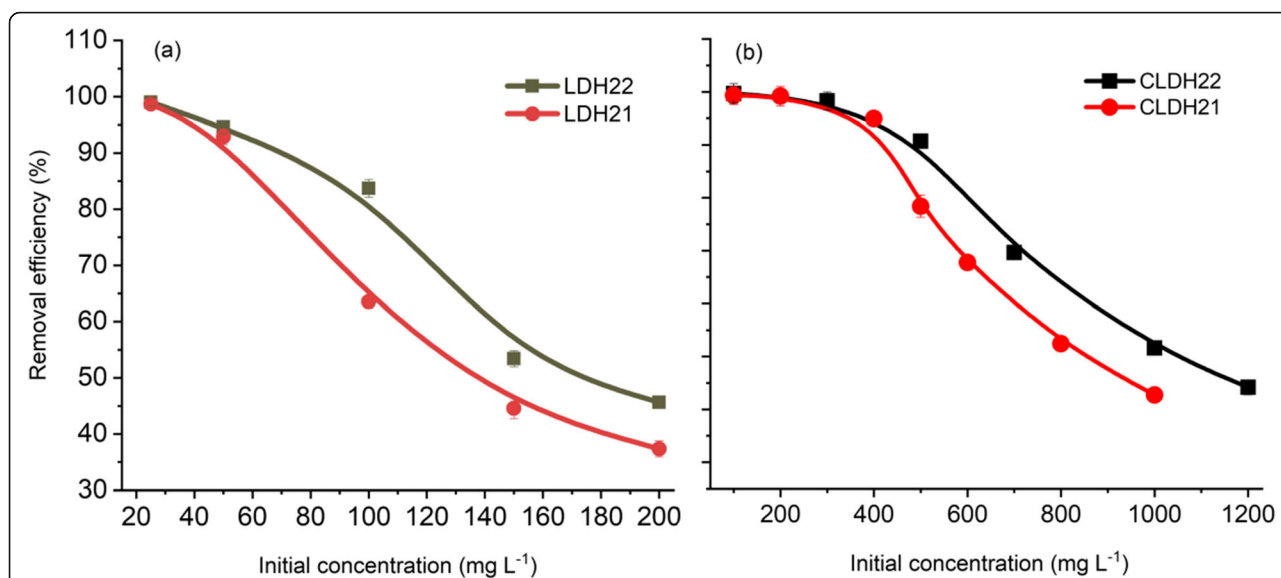


Fig. 7 Effect of initial concentration on removal efficiency of IDB onto LDHs (a) and CLDHs (b) adsorbent

of the sorption and the nonlinearity degree between concentration and sorption, respectively.

The adsorption isotherm models; Langmuir and Freundlich’s parameters for IDB sorption onto LDHs and CLDHs sorbent are recorded in Table 4. The R_L ($0 < R_L < 1$) confirms a favorable sorption process. The n values within range 1 and 10 that represent a good sorption potential of the sorbent, that is indicative of surface heterogeneity [36].

The experimental data confirm that the sorption behaviors of IDB dye onto LDHs and CLDHs could be better represented by the Langmuir’s isotherm in concentration range studied (coefficient of determination, R^2 (0.992–0.999)). This also demonstrates that IDB dye is sorbed onto sorbents as monolayer adsorption. The n values of IDB dye onto LDHs and CLDHs lie in the range from 4.72 to 5.65 as shown in Table 4. This refers to that, IDB dye could be easily sorbed on the different layered double hydroxide sorbents either as synthesized or calcined. Consequently, the theoretical maximum capacity, q_{cal} estimated from Langmuir’s isotherm was found to be 74, 90, 427 and 529 mg g^{-1} , for

LDH21, LDH22, CLDH21 and CLDH22, respectively, that are close to the experimental data, $q_{max(exp)}$: 75, 91, 427 and 530 mg g^{-1} or 12, 14.7, 68.6 and 85.1 mmol per 100 g, respectively. The obtained sorption capacity of the best sorbent in the present study, CLDH22, is apparently higher than the reported results for recent CLDHs such as Mg-Fe, NiFe [16, 27].

Temperature effect

Temperature effect on IDB sorption capacity onto CLDH22 as a representative for the studied sorbents is presented in Fig. 8. It was found that, the sorption capacity increases with raising temperature. The enhanced removal of IDB ions onto CLDH22 adsorbent may be due to the increase of IDB ions mobility, the swelling of pore structure of the adsorbent and decrease of the retarding forces between the adsorbate ions and adsorbent [33].

Determination of the thermodynamic parameters

The sorption thermodynamic parameters were estimated using Van’t Hoff’s Eq. (12) and the values are listed in Table 5:

Table 4 Langmuir and Freundlich’s parameters for IDB adsorption onto LDHs and CLDHs adsorbent

Adsorbent	q_{max} (exp) (mg g^{-1})	Langmuir parameters				Freundlich parameters		
		q_{max} (cal) (mg g^{-1})	R_L	b_L (L mg^{-1})	R^2	k_F	$1/n$	R^2
LDH21	75	74	0.016–0.118	0.30	0.992	32.5	0.18	0.951
LDH22	91	90	0.011–0.082	0.445	0.992	36.6	0.21	0.904
CLDH21	427	427	0.005–0.049	0.195	0.999	150.5	0.19	0.793
CLDH22	530	529	0.006–0.069	0.135	0.999	162.4	0.21	0.869

b_L is the Langmuir adsorption constant (L mg^{-1}). k_F is a roughly indicator of the adsorption capacity and $1/n$ is the adsorption intensity

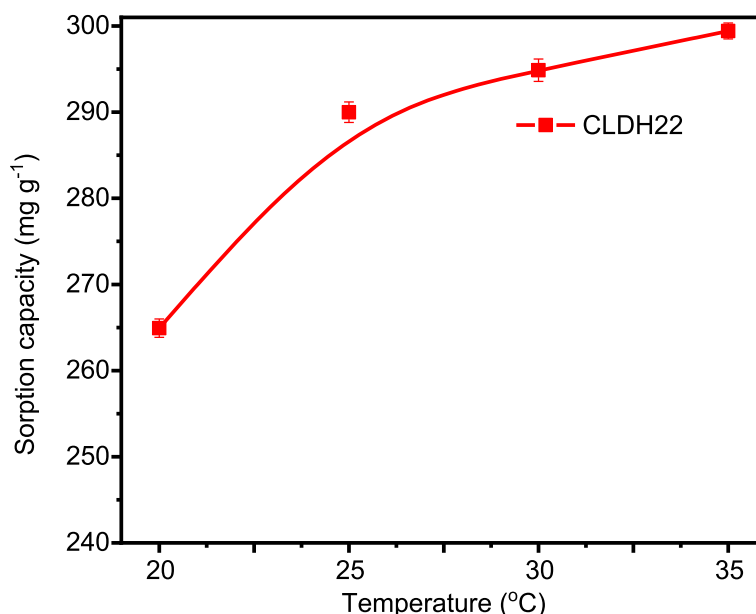


Fig. 8 Effect of temperature on adsorption capacity of IDB onto CLDH22 adsorbent, $C_i = 300 \text{ mg L}^{-1}$

$$\ln K_d = \frac{\Delta S_{\text{sorption}}}{R} - \frac{\Delta H_{\text{sorption}}}{RT} \tag{12}$$

$$\Delta G_{\text{sorption}} = \Delta H_{\text{sorption}} - T\Delta S_{\text{sorption}} \tag{13}$$

where, K_d is the distribution coefficient that is equal to q_e/C_e and R is the molar gas constant ($8.314 \text{ J mol}^{-1} \text{ K}^{-1}$), $\Delta G_{\text{adsorption}}$, $\Delta H_{\text{adsorption}}$ and $\Delta S_{\text{adsorption}}$ are the changes in adsorption free energy, enthalpy and entropy, respectively.

The values of $\Delta G_{\text{adsorption}}$ are negative, indicating that the IDB dye ions sorption onto CLDH22 is a spontaneous and thermodynamically favorable. The more negative values of $\Delta G_{\text{adsorption}}$ indicate a greater driving force to the sorption process.

The value of $\Delta H_{\text{adsorption}}$ is positive confirming that the sorption process is endothermic process. Generally, the value of $\Delta H_{\text{adsorption}}$ for the physical adsorption is $< 20 \text{ kJ mol}^{-1}$, whereas the chemisorption is within the range $85\text{--}200 \text{ kJ mol}^{-1}$ [37]. The obtained value of

$\Delta H_{\text{adsorption}}$ (200 kJ mol^{-1}) for this case is indicating that the process is organized by a spontaneous chemisorption process which is in covenant with the suggested intercalation mechanism of IDB ions in the Van der Waal's gap [17].

The positive value of $\Delta S_{\text{adsorption}}$ may be due to the increase in randomness through intercalation of IDB dye on CLDH22 according to Eq. (13). The increase in randomness also arises from the recovery of the LDH structure in the so-called 'memory effect' when contacted with IDB solution. The conclusion from these results is that the endothermic sorption is entropically driven.

A comparison between uptake capacities of recent LDHs or CLDHs and common sorbents towards sulfonated dyes is presented in Table 2. It appears that, CLH22 is characterized by relatively high capacity and fast kinetics of IDB dye adsorption.

Desorption study

Table 6 shows desorption results of IDB-loaded onto LDHs or CLDHs using different eluents NaCl, NaOH or Na_2CO_3 with a concentration 0.1 or 1.0 M, respectively, at 30 or 55 °C. The elution efficiency order of IDB dye from LDHs and CLDHs was $\text{Na}_2\text{CO}_3 > \text{NaOH} > \text{NaCl}$, that confirms the relative intercalation preferences of their anions. This was due to the high degree of affinity of carbonate for LDHs [32]. Also, by raising the applied temperature of desorption from 30 to 55 °C the release of the loaded IDB increased.

Table 5 The thermodynamic parameters of IDB adsorption onto CLDH22 adsorbent, $C_i = 300 \text{ mg L}^{-1}$

Adsorbent	T (K)	ΔH_{ads} (kJ mol^{-1})	ΔS_{ads} ($\text{kJ K}^{-1} \text{ mol}^{-1}$)	ΔG_{ads} (kJ mol^{-1})	R^2
CLDH22	293	200	0.70	-4.71	0.927
	298			-8.20	
	303			-11.7	
	308			-15.2	

Table 6 Desorption study of IDB-loaded onto LDHs and CLDHs at 30 and 50 °C

Eluent	Concentration of eluent, mol L ⁻¹	Eluted IDB (%) at 30 °C				Eluted IDB (%) at 50 °C			
		LDH21	LDH22	CLDH21	CLDH22	LDH21	LDH22	CLDH21	CLDH22
NaCl	0.1	6.6	2.9	2.6	0.9	18	9.2	6.6	1.7
NaOH	0.1	17	10	4.0	1.9	29	15	10	4.3
Na ₂ CO ₃	0.1	26	17	8.8	3.0	36	22	15	7.1
Na ₂ CO ₃	1.0	39	22	15	5.1	50	25	27	10

The lower percentage of the recovered dye from IDB-CLDHs compared with IDB-LDHs may be attributed to the better orientation of IDB inside the sheets of CLDHs with the intercalation mechanism and the higher uptake of the dye. The possibility of release of the loaded dye from the sorbents ensures that they will not be a secondary waste material on application, as they can be purified.

Application

Removal of IDB dye

The removal process of IDB dye waste that produced from the simulated dyeing process was applied onto the effective sorbents; LDH22 and CLDH22 with an initial concentration 100 and 400 mg L⁻¹, respectively, at optimum pH 4.3. The obtained removal efficiencies were 97 and 81% for CLDH22 and LDH22 sorbents, respectively.

Conclusions

The newly reported layered double hydroxides LDH21 and LDH22 and its calcined products CLDH21 and CLDH22 were evaluated as potential sorbents for IDB. It was optimally extracted at pH 4.3 after 3 h of shaking. The complete removal (> 99%) of IDB was achieved at adsorbent dosage 2.0 g L⁻¹ of the investigated samples except LDH21 3.0 g L⁻¹. The sorption process was found to follow the pseudo 2nd order kinetic and Langmuir-type sorption isotherm with a monolayer capacities of 75–530 mg g⁻¹ of IDB dye onto LDHs and CLDHs. The measured thermodynamic parameters $\Delta G_{adsorption}$, $\Delta H_{adsorption}$ and $\Delta S_{adsorption}$ of IDB onto the best adsorbent CLDH22 confirmed that the sorption process of IDB was spontaneous and endothermic chemisorption in nature. FTIR, SEM and S_{BET} measurements confirmed the LDH structure of LDH22 and the loading of IDB. The magnetic separation of IDB anions onto Fe-containing sorbents were demonstrated which may facilitate the separation process on application. The magnetic separation of IDB anions onto Fe-containing sorbents were demonstrated which may facilitate the subsequent separation process. 1 M Na₂CO₃ solution was considered the most efficient eluent for loaded IDB from LDHs and CLDHs at 50 °C. CLDH22 and LDH22 sorbents were evidenced as potential sorbents for the remediation of an

IDB-contaminated simulated dyeing effluent with removal efficiencies 97 and 81%, respectively.

Dedication

It is our genuine gratefulness and warmest regard that we dedicate this work to the sole of Prof. Dr. Medhat A. H. Hafez and Prof. Dr. Ibrahim M. M. Kenawy for their devotion and guidance.

Acknowledgements

The authors deeply thank Mr. Hamdy Abdel Sadek, DyStar, Egypt, for his advice and cooperation.

Authors' contributions

IK, MH, AM and KA suggested the point. ZAE carried out experimental. IK, MH, AM, ZAE and KA contributed in discussion. ZAE wrote the paper. IK, MH, AM, ZAE and KA revised the paper.

Funding

N/A

Availability of data and materials

All data generated or analyzed during this study can be obtained from the corresponding author.

Declarations

Competing interests

The authors declare they have no competing interests.

Author details

¹Department of Chemistry, Mansoura University, Mansoura 35516, Egypt. ²Textile Research Division, National Research Centre, Giza 12622, Egypt. ³Inorganic Chemistry Department, National Research Centre, Giza 12622, Egypt.

Received: 18 June 2020 Accepted: 10 September 2021

Published online: 14 October 2021

References

1. Dragan ES, Humelnicu D. Erratum: Dragan, E.S., et al., Contribution of cross-linker and silica morphology on Cr (VI) sorption performances of organic anion exchangers embedded into silica pores. *Molecules*. 2020;25:2736.
2. Raj SI, Jaiswal A, Uddin I. Tunable porous silica nanoparticles as a universal dye adsorbent. *RSC Adv*. 2019;9:11212–9.
3. Kalpana D, Shim JH, Oh BT, Senthil K, Lee YS. Bioremediation of the heavy metal complex dye Isolan Dark Blue 2SGL-01 by white rot fungus *Irpex lacteus*. *J Hazard Mater*. 2011;198:198–205.
4. Figgitt M, Newson R, Leslie IJ, Fisher J, Ingham E, Case CP. The genotoxicity of physiological concentrations of chromium (Cr (III) and Cr (VI)) and cobalt (Co (II)): an *in vitro* study. *Mutat Res-Fund Mol M*. 2010;688:53–61.
5. Isosaari P, Srivastava V, Sillanpaa M. Ionic liquid-based water treatment technologies for organic pollutants: current status and future prospects of ionic liquid mediated technologies. *Sci Total Environ*. 2019;690:604–19.
6. Wu AM, Zhao XL, Wang JY, Tang Z, Zhao TH, Niu L, et al. Application of solid-phase extraction based on magnetic nanoparticle adsorbents for the

- analysis of selected persistent organic pollutants in environmental water: a review of recent advances. *Crit Rev Env Sci Tec.* 2021;51:44–112.
7. Evans DG, Slade RCT. Structural aspects of layered double hydroxides. *Struct Bond.* 2006;119:1–87.
 8. Zumreoglu-Karan B, Ay AN. Layered double hydroxides - multifunctional nanomaterials. *Chem Pap.* 2012;66:1–10.
 9. Radha S, Navrotsky A. Energetics of CO₂ adsorption on Mg–Al layered double hydroxides and related mixed metal oxides. *J Phys Chem C.* 2014; 118:29836–44.
 10. Lei CS, Zhu XF, Zhu BC, Jiang CJ, Le Y, Yu JG. Superb adsorption capacity of hierarchical calcined Ni/Mg/Al layered double hydroxides for Congo red and Cr (VI) ions. *J Hazard Mater.* 2017;321:801–11.
 11. Ling FL, Fang L, Lu Y, Gao JM, Wu F, Zhou M, et al. A novel Co/Fe layered double hydroxides adsorbent: high adsorption amount for methyl orange dye and fast removal of Cr (VI). *Micropor Mesopor Mat.* 2016;234:230–8.
 12. Bu R, Chen FF, Li J, Li W, Yang F. Adsorption capability for anionic dyes on 2-hydroxyethylammonium acetate-intercalated layered double hydroxide. *Colloid Surface A.* 2016;511:312–9.
 13. Shan RR, Yan LG, Yang YM, Yang K, Yu SJ, Yu HQ, et al. Highly efficient removal of three red dyes by adsorption onto Mg-Al-layered double hydroxide. *J Ind Eng Chem.* 2015;21:561–8.
 14. Chakraborty P, Nagarajan R. Efficient adsorption of malachite green and Congo red dyes by the surfactant (DS) intercalated layered hydroxide containing Zn²⁺ and Y³⁺-ions. *Appl Clay Sci.* 2015;118:308–15.
 15. Wang SM, Li ZH, Lu C. Polyethyleneimine as a novel desorbent for anionic organic dyes on layered double hydroxide surface. *J Colloid Interf Sci.* 2015; 458:315–22.
 16. Peng C, Dai J, Yu JY, Yin J. Calcined Mg-Fe layered double hydroxide as an adsorbent for the removal of methyl orange. *AIP Adv.* 2015;5:057138.
 17. Liji Sobhana SS, Mehedí R, Malmivirta M, Paturi P, Lastusaari M, Durtu MM, et al. Heteronuclear nanoparticles supported hydrotalcites containing Ni (II) and Fe (III) stable photocatalysts for Orange II degradation. *Appl Clay Sci.* 2016;132-3:641–9.
 18. Abou-El-Sherbini KS, Kenawy IMM, Hafez MAH, Lotfy HR, AbdElbary ZMEA. Synthesis of novel CO₃²⁻/Cl⁻-bearing 3(Mg + Zn)/(Al + Fe) layered double hydroxides for the removal of anionic hazards. *J Environ Chem Eng.* 2015;3: 2707–21.
 19. Fleming I, Williams D. *Spectroscopic methods in organometallic chemistry.* 7th ed. Cham: Springer; 2019.
 20. Hafez MAH, Kenawy IMM, Abd Elbary ZME, Elmorsi RR, Abou-El-Sherbini KS. Removal of Cr (VI) from aqueous media on calcined (Mg-Zn)/(Al-Fe)-(CO₃)/Cl layered double hydroxides. *Desalin Water Treat.* 2019;148:270–84.
 21. Olf HW, Torres-Dorante LO, Eckelt R, Kosslick H. Comparison of different synthesis routes for Mg-Al layered double hydroxides (LDH): characterization of the structural phases and anion exchange properties. *Appl Clay Sci.* 2009; 43:459–64.
 22. Mokhtar M, Inayat A, Ofili J, Schwiager W. Thermal decomposition, gas phase hydration and liquid phase reconstruction in the system Mg/Al hydrotalcite/ mixed oxide: a comparative study. *Appl Clay Sci.* 2010;50:176–81.
 23. Saiah FBD, Su BL, Bettahar N. Nickel-iron layered double hydroxide (LDH): textural properties upon hydrothermal treatments and application on dye sorption. *J Hazard Mater.* 2009;165:206–17.
 24. Seida Y, Nakano Y. Removal of phosphate by layered double hydroxides containing iron. *Water Res.* 2002;36:1306–12.
 25. Klopogge J. The kaolin group: hydroxyl groups. In: *Spectroscopic methods in the study of kaolin minerals and their modifications.* Cham: Springer; 2019. p. 41–96.
 26. Abdelkader NBH, Bentouami A, Derriche Z, Bettahar N, de Menorval LC. Synthesis and characterization of Mg-Fe layer double hydroxides and its application on adsorption of Orange G from aqueous solution. *Chem Eng J.* 2011;169:231–8.
 27. Lei CS, Pi M, Kuang PY, Guo YQ, Zhang FG. Organic dye removal from aqueous solutions by hierarchical calcined Ni-Fe layered double hydroxide: isotherm, kinetic and mechanism studies. *J Colloid Interf Sci.* 2017;496:158–66.
 28. Vahidhabanu S, Karuppasamy D, Adeogun AI, Babu BR. Impregnation of zinc oxide modified clay over alginate beads: a novel material for the effective removal of congo red from wastewater. *RSC Adv.* 2017;7:5669–78.
 29. Sharifzade G, Asghari A, Rajabi M. Highly effective adsorption of xanthene dyes (rhodamine B and erythrosine B) from aqueous solutions onto lemon citrus peel active carbon: characterization, resolving analysis, optimization and mechanistic studies. *RSC Adv.* 2017;7:5362–71.
 30. Lagergren S. About the theory of so-called adsorption of dissolved substances. *Handlingar.* 1898;24:1–39 [in German].
 31. Ho YS, McKay G. Pseudo-second order model for sorption processes. *Process Biochem.* 1999;34:451–65.
 32. Weber WJ, Morris JC. Kinetics of adsorption on carbon from solution. *J Sanit Eng Div.* 1963;89:31–60.
 33. Mezenner NY, Bensmaili A. Kinetics and thermodynamic study of phosphate adsorption on iron hydroxide-eggshell waste. *Chem Eng J.* 2009;147:87–96.
 34. Langmuir I. The adsorption of gases on plane surfaces of glass, mica and platinum. *J Am Chem Soc.* 1918;40:1361–403.
 35. Freundlich H. Over the adsorption in solution. *J Phys Chem.* 1907;57:385–470 [in German].
 36. Foo KY, Hameed BH. Insights into the modeling of adsorption isotherm systems. *Chem Eng J.* 2010;156:2–10.
 37. Liu Y, Liu Y. Biosorption isotherms, kinetics and thermodynamics. *Sep Purif Technol.* 2008;61:229–42.

Publisher's Note

Springer Nature remains neutral with regard to jurisdictional claims in published maps and institutional affiliations.

Ready to submit your research? Choose BMC and benefit from:

- fast, convenient online submission
- thorough peer review by experienced researchers in your field
- rapid publication on acceptance
- support for research data, including large and complex data types
- gold Open Access which fosters wider collaboration and increased citations
- maximum visibility for your research: over 100M website views per year

At BMC, research is always in progress.

Learn more biomedcentral.com/submissions

